Elucidation of the Hydrogen Evolution Reaction on a Photochemical Molecular Device

Axel Gross

axel.gross@uni-ulm.de

University of Ulm https://orcid.org/0000-0003-4037-7331

Miftahussurur Putra

University of Ulm

Alexander Mengele

University of Ulm

Benedikt Bagemihl

University of Ulm

Sven Rau

University of Ulm

Michael Busch

Lulea University of Technology

Article

Keywords: photocatalyst, hydrogen evolution reaction, density functional theory, homogeneous catalysis

Posted Date: September 26th, 2025

DOI: https://doi.org/10.21203/rs.3.rs-5775846/v1

Additional Declarations: There is **NO** Competing Interest.

Elucidation of the Hydrogen Evolution Reaction on a Photochemical Molecular Device

Miftahussurur Hamidi Putra,[†] Alexander K. Mengele,[‡] Benedikt Bagemihl,[‡] Sven Rau,[‡] Michael Busch,[†,¶,§] and Axel Groß[*,†,‖]

†Institute of Theoretical Chemistry, Ulm University, 89081 Ulm, Germany

‡Institute of Inorganic Chemistry I, Materials and Catalysis, Ulm University, 89081 Ulm, Germany

¶Division of Materials Science, Department of Engineering Sciences and Mathematics, Luleå University of Technology, 971 87 Luleå, Sweden

§Wallenberg Initiative Materials Science for Sustainability (WISE), Luleå University of Technology, 971 87 Luleå, Sweden

‖Helmholtz Institute Ulm (HIU), Electrochemical Energy Storage, 89069 Ulm, Germany

E-mail: axel.gross@uni-ulm.de

Abstract

One of the ultimate goals of photocatalysis is the direct utilzation of solar energy into the production of useful chemical products. In particular the direct photocatalytic water splitting to produce molecular hydrogen as a versatile, sustainable and ecologically friendly fuel is of great interest. This goal has motivated numerous research efforts to develop and improve corresponding photochemical molecular devices. However, it is fair to say that most of these efforts concentrated on the identification of the light-driven electron transfer processes within these devices, whereas the mechanistic details

of the hydrogen evolution reaction remained largely unexplored. Here we present a first-principles based theoretical study of a photochemical molecular device that combines the determination of the light-driven electron transfer processes with the elucidation of the mechanistic details of the photo-induced hydrogen evolution reaction.

Keywords

photocatalyst, hydrogen evolution reaction, density functional theory, homogeneous catalysis

Introduction

Green H_2 is considered an important energy carrier for the necessary future industrial transformation.[1–4] However, the efficient and sustainable production of molecular hydrogen still represents a severe challenge. Photochemical molecular devices for the photocatalytic hydrogen evolution, which integrate photoredox active photosensitizer and catalyst units linked by a bridging ligand[5–15] represent a promising alternative to the traditional combination of separate photovoltaic devices and electrocatalysts for the hydrogen evolution reaction (HER).

Among these photochemical molecular devices, $[(tbbpy)_2Ru(tpphz)PtI_2]^{2+}$ (tbbpy = 4,4′-di-*tert*-butyl-2,2′-bipyridine, tpphz = tetrapyrido [3,2-a:2′,3′-c:3‴′-h:2‴,3‴-j] phenazine) or simply $RuPtI_2$ has shown a great promise for photocatalytic hydrogen evolution.[9,16,17] $RuPtI_2$ consists of a Ru polypyridyl unit which acts as photosensitizer and a PtI_2 catalyst. Both units are connected by a tpphz bridge.[16,17] Previous measurements showed remarkable HER activity for this complex. A turnover number (TON) exceeding 450 was observed in mixtures of acetonitrile (MeCN), water, and triethylamine (NEt_3) in a volumetric composition of 6:1:3.[17] To the best of our knowledge, this result represents one of the highest photocatalytic hydrogen gas production yield among photochemical molecular devices utilizing a platinum-based catalysts. In addition, $RuPtI_2$ shows not only high photocatalytic per-

formance, but also exhibits good stability as a catalyst under operational conditions.[12,16,17] Beyond its high stability, RuPtI2 can be repaired by different pathways, which reinvigorate its photocatalytic capacity.[17,18] This very rare capability renders a detailed understanding of its actual photocatalytic mechanism very important.

Although the electron transfer mechanism during the photocatalytic process of $RuPtI_2$ is well-studied,[16,17,19–21] the understanding of the hydrogen production mechanism still remains incomplete. To the best of our knowledge, only few studies have explored the mechanistic aspects of hydrogen production in Pt-based molecular catalysts.[22,23] They suggest that for [(bpy)PtX_2] catalysts (bpy = 2,2'-bipyridine) HER likely proceeds via a dimeric Pt···Pt–H intermediate. However, their theoretical investigation is limited to catalytic complexes thus not considering the full photochemical molecular device with the catalyst and the photosensitizer being included within one large photocatalytic molecule. Furthermore, only the thermochemistry but no complete reaction paths have been determined.

As photo- and electrochemistry likely share many mechanistic similarities, it is worthwhile considering aspects of the electrocatalytic HER. Here, the first step typically consists of the Volmer step[24]

$$\text{Volmer} : * + \ \mathrm{H^+} + e^- \longrightarrow \mathrm{H}* \ , \tag{1}$$

which corresponds to the reductive adsorption of a proton from the electrolyte on the active site of the catalyst denoted by $*$. To complete the HER, there are two possible mechanisms, either the Volmer-Tafel mechanism involving a chemical recombination reaction or the Volmer-Heyrovsky mechanism involving a second charge-transfer step:[24–32]

$$\text{Tafel} : 2\mathrm{H}* \longrightarrow 2 * + \ \mathrm{H_2} \tag{2a}$$

$$\text{Heyrovsky} : \mathrm{H} * + \ \mathrm{H^+} + e^- \longrightarrow * + \ \mathrm{H_2} \tag{2b}$$

As these reaction schemes show, the HER is a coupled two-electron two-proton process.

Although there are experimental techniques to determine the kinetic parameter of the HER,[33] it is hardly possible to identify the exact reaction sites, the microscopic reaction mechanism and possible reaction intermediates. Spectroscopic investigations are often limited to the initial one-electron transfer steps, measurements under operando conditions are difficult to implement and critical intermediates lack suitable spectroscopic signatures. Consequently, other strategies to identify the HER mechanism are asked for. This task is herein tackled by the quantum chemical description of an overall mechanism for the light-driven HER of the $RuPtI_2$ photochemical molecular device utilizing a detailed determination of electron excitation and transfer mechanisms, reaction energetics and activation barriers.

In detail, we have employed density functional theory (DFT) to investigate the potential intermediates involved in the reaction. In adddition, time-dependent density functional theory (TD-DFT) has been utilized to comprehensively analyze the excitation properties of the intermediates during the photocatalytic process. By following this approach, we not only gain unprecedented insights into the mechanism of the hydrogen evolution from $RuPtI_2$, but also elucidate how this photocatalyst molecule protects itself from degradation. Understanding this mechanism is invaluable for future advancements in developing photochemical molecular devices to achieve optimal hydrogen production.

Computational Details

In this work, we investigate the potential intermediates involved in the photocatalytic HER of $RuPtI_2$ using DFT calculations. We started our investigation by scanning the possible configuration of $RuPtI_2$ photocatalyst under reaction conditions. Our calculation also includes the careful analysis of different charge and spin states. All DFT calculations were performed using the Gaussian 16 Rev C.01 code.[34] The B3LYP functional[35,36] together with Grimme DFT-D3 dispersion corrections and Becke-Johnson damping[37] in combination with a def2-SVP basis set[38,39] has been employed for the geometry optimization. Afterwards,

single point calculations at the relaxed geometries using the same functional but a larger def2-TZVP basis set[38,39] have been performed to obtain converged energies on the single-particle level.

The theoretical modeling of electrocatalytic processes requires an appropriate consideration of the interface between the catalyst and the electrolyte.[40] As the solvent we have considered acetonitrile which has also been used in corresponding experiments.[17,18] To model the solvent, we employed here the solvation model based on density (SMD).[41] We neglected the influence of water and NEt_3 on the solvent properties, such as the dielectric constant, as it has been shown that this mixture does not affect the optical properties of $RuPtI_2$.[17] In addition, TD-DFT[42,43] has been utilized to comprehensively analyze the excitation properties of the intermediates during the photocatalytic process. For the TD-DFT calculations, we employed the same setup as used in the geometry optimization.

To assess the probability of proton binding to the photochemical molecular device, we derived values of the acid dissociation constant pK_a from the calculated proton solvation energies using the isodesmic method.[44–50] Based on our calculations, the proton solvation energy value in acetonitrile is -11.20 eV which compares well with previously measured and calculated values.[51,52] For details of the method for calculating the proton solvation energy and pK_a we refer to the Supplementary Information (SI) and the literature.[45,53] Finally, the reduction energy of the $RuPtI_2$ is determined from DFT calculations using the NEt_3/NEt_3^+ redox couple as reference.

Results and Discussion

As illustrated in the Volmer-Tafel (Eqs. 1 and 2a) and the Volmer-Heyrovsky (Eqs. 1 and 2b) mechanisms, the electrocatalytic HER requires the transfer of to two electrons to the two protons. These electrons have to be provided by the electrocatalyst. Without irradation, the $RuPtI_2$ complex is inactive with respect to the HER. Thus the catalytic activity of

the $RuPtI_2$ complex has to be initiated by the photoinduced electron transfer from the photoactive Ru center of the complex to its PtI_2 catalyst. Thus our quest for the elucidation of the microscopic steps in the photo-induced HER of the $RuPtI_2$ complex was performed as a search for possible electron- and proton-transfer steps guided by experimental spectroscopic information where available.[16,17,19–21]

With respect to the chemical environment the $RuPtI_2$ complex is dissolved in, challenges do not only arise from the unknown solvent properties of the acetonitrile, water, and NEt_3 mixture but are also caused by the unknown pH value of electrolyte under catalytic conditions. Therefore, we first discuss the calculated pK_a values of the three protonated species H_3O^+, NEt_3H^+, and $MeCNH^+$ in acetonitrile. Our DFT calculations reveal that H_3O^+ and $MeCNH^+$ have low pK_a values of -7.2 and -2.2, respectively. Water can also be excluded as a proton donor since earlier studies indicate that its pK_a in acetonitrile rises, owing to the poor stabilization of OH^-, to 40.[45,46] As a result, water and acetonitrile are predominately not protonated under reaction conditions. In contrast, NEt_3H^+ displays a pK_a of 17.6 which is satisfactorily close to the experimental value of 18.8.[54] Consequently, for the HER on $RuPtI_2$ to occur, the pK_a value of the metal hydride at $RuPtI_2$ must be higher than 17.6, otherwise the protons would hardly bind to the photocatalyst. Based on this requirement, we constructed all reasonable reaction pathways for the light-driven HER at $RuPtI_2$.

The complete proposed catalytic cycle of the light-driven HER on $RuPtI_2$ is depicted in Scheme 1. In its electronic ground state, $RuPtI_2$ is inactive towards the HER as it has a highly acidic pK_a of -4.7 at the PtI_2-catalyst. The nitrogen atoms on the bridging ligand represent additional possible protonation sites. However, they also have low pK_a values of 3.2 and -4.4 for the first and second protonation on the bridge, respectively, so that no protons are bound to $RuPtI_2$ in its electronic ground state.

The HER is initiated by the reductive activation of $RuPtI_2$ through the initial electronic excitation to state **1*** requiring an energy of *ca.* 2.85 eV (λ = 435 nm, S17, see Scheme 2). This excitation corresponds to a singlet metal-to-ligand charge transfer (^{1}MLCT) involving

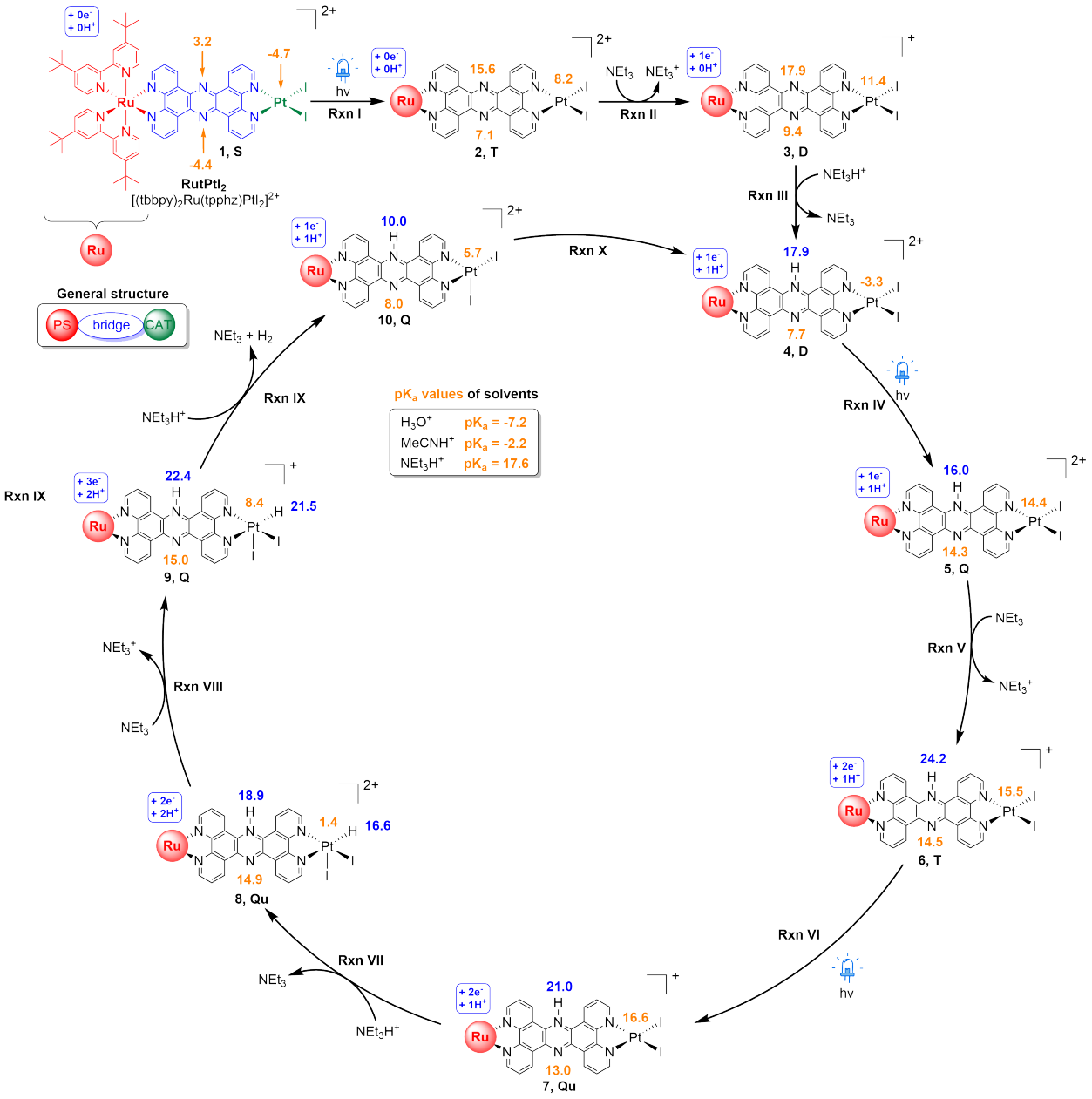

Scheme 1: Overall reaction mechanism of light-driven hydrogen evolution reaction with $RuPtI_2$. Numeric labeling of intermediates along with their spin states (S = singlet, D = doublet, T = triplet, Q = quartet, Qu = quintet) is given in black below each species. pK_a values of the N and Pt sites of the respective intermediates are given in orange color whereas the pK_a values of the deprotonation of already occupied hydrogen sites are printed in blue. The total number of electrons and protons stored at $RuPtI_2$ is given in blue boxes. Abbreviations: photosensitizer (PS), catalyst unit (CAT). Top left: Molecular structure of $RuPtI_2$ and general design concept for intramolecularly operating photocatalysts.

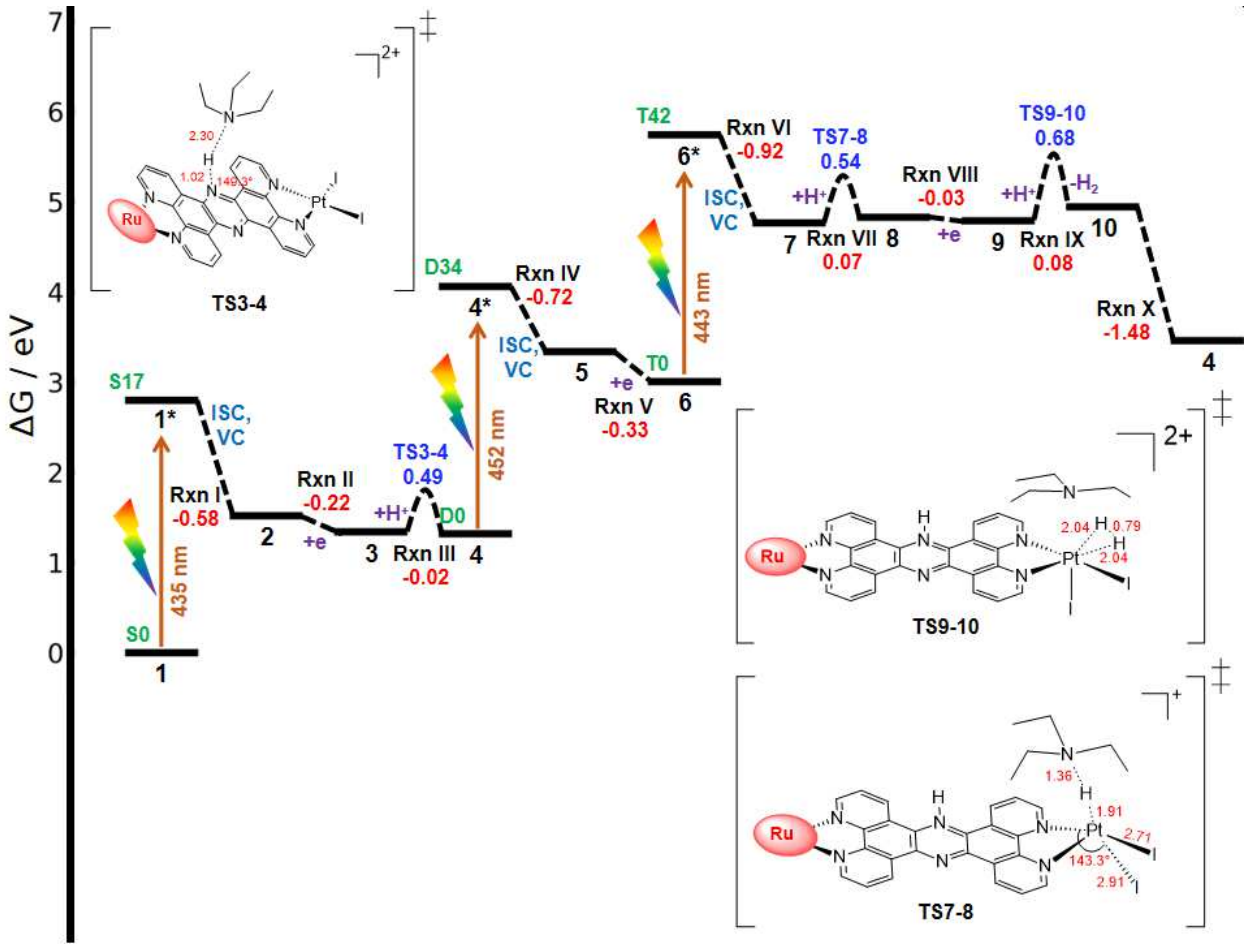

Scheme 2: Reaction energetics along the catalytic cycle shown in Scheme 1. The reaction energies are shown in red color, the activation energies of selected steps are printed in blue, all energies are given in eV. Here, NEt_3H^+ is considered as the proton source. In addition, the structure of the three major transition states is illustrated with the bipyridine ligands being removed for the sake of clarity.

electron transfer from the ruthenium metal center to the ligands (see Figure 1a). Afterwards, the excitation process is followed by an intersystem crossing (ISC) and vibrational relaxation to form intermediate **2**. This intermediate differs only in the spin state and electron distribution from the intermediate **1**. It corresponds to a ^{3}MLCT state with excess electron density at the tpphz ligand. In the MLCT, approximately 0.7e are shifted from the photosensitizer (ruthenium and bipyridine ligand) to the tpphz bridge (see Mulliken charge and spin state in Figure S1 and S2). As the next step, the sacrificial electron donor triethylamine (NEt_3) donates an electron to intermediate **2**, as experimentally well-known,[55–59] with $\Delta G = -0.22$

eV and thus reduces the photocatalytic molecule to produce the intermediate **3**, as shown in Rxn II, where the excess of the electron is accumulated at the bridge (see Figure S1 and S2). The probability of Pt-H bond formation in intermediate **2** and **3** is very low due to their pK_a values being approximately 9 and 6 units lower than that of NEt_3H^+, respectively. Therefore, both intermediates cannot be considered as active species in the photocatalytic process.

However, one of the nitrogen atoms in the bridging ligand of intermediate **3** possesses a pK_a of 17.9 which is larger than the pK_a of NEt_3H^+. Consequently, the proton transfer from NEt_3H^+ to form the intermediate **4** is slightly exothermic, only hindered by a moderate energy barrier of 0.49 eV. This process is slightly more favorable than the bridge protonation of intermediate **2** with an activation barrier of 0.56 eV. According to our calculation, upon activation the structure of NEt_3H^+ becomes modified to avoid the steric interaction with $RuPtI_2$ resulting in a **TS3-4** transition state geometry with a N−H bond length of 1.02 Å and a bond angle of 149.3° relative to the plane of the bridging ligand (see Scheme 2). This particular mechanism proceeding through intermediate **4** is in good agreement with the experimental findings,[17,18,21] thus confirming that the single protonation of the bridging ligand is an intermediate step in the photocatalytic process.

According to our determination of the pK_a values, intermediate **4** remains inactive for any HER step, since this intermediate has a highly acidic pK_a value of -3.3 for the protonated Pt center. Furthermore, the second protonation of the bridging ligand of intermediate **4** is associated with a pK_a of 9.4 which is still lower than the pK_a of NEt_3H^+. According to experiments,[8,16–18,21,60] a significant decline in the catalytic activity is observed once spectroscopy results indicate a two-fold protonation of the bridging ligand.[17] Obviously, the fully protonated bridging ligands correspond to the deactivated state. According to our calculations, the deactivation of the photocatalyst should not occur after reaction step Rxn III. In order to understand this, we highlight the role of the sacrificial electron donor (NEt_3) used in this reaction. Beyond its function as an electron supplier, the basic pK_a value 17.6 of

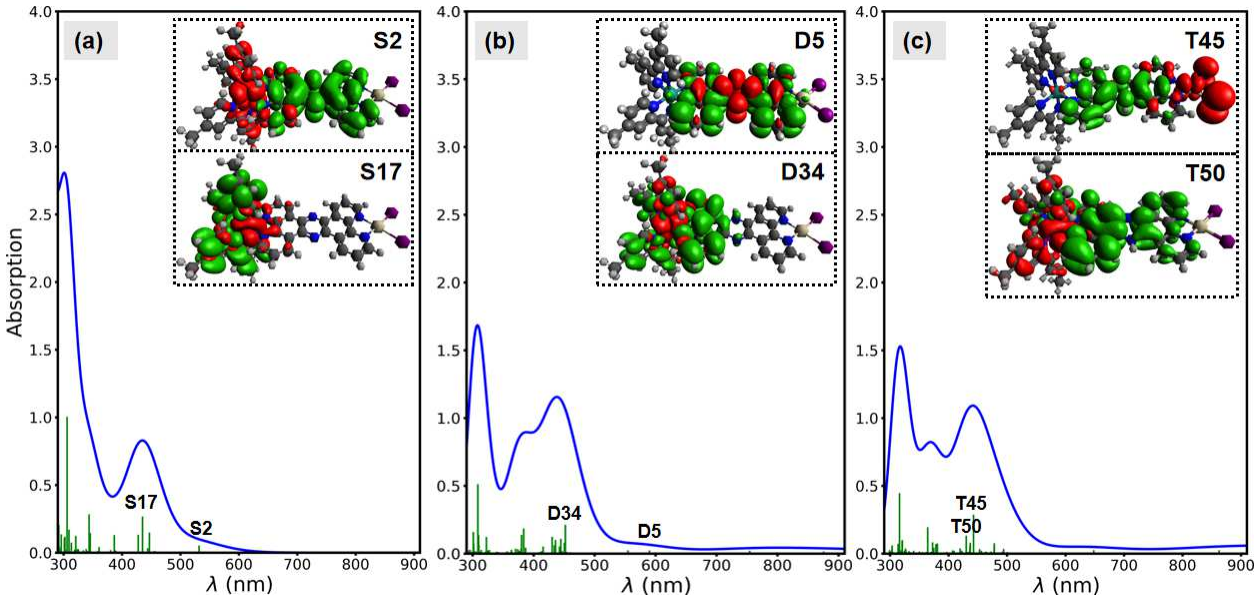

Figure 1: Absorption spectra of the intermediates **1** (panel a), **4** (b), and **6** (c). In addition, the most important excited states together with their excitation induced charge density difference are shown. The excitation direction corresponds to the transition from red to green.

NEt_3H^+ also serves as a proton regulator. If an electron donor with a lower pK_a value of, say, 9.0 is chosen, the $RuPtI_2$ in its intermediate state **4** would become deactivated by the second protonation of the bridging ligand.

Furthermore, we found from the TD-DFT calculations that the oscillator strength of the ligand to metal charge transfer (LMCT) from the bridging ligand to the $d_{x^2-y^2}$ orbital of the Pt-catalyst in the intermediate configurations **3** and **4** is zero (see Table S3 and S4). As a result, the LMCT process may not occur at all or will proceed very slowly. This has been demonstrated by performing photoelectrochemistry measurements by Müller and coworkers on the reduced form of $RuPtI_2$.[21] Based on this work, the excitation process of the reduced $RuPtI_2$ ends with charge accumulation on the bipyridine moiety bound to the catalyst,[21] instead of on the Pt-catalyst itself. Therefore, it can be concluded that the LMCT process in the intermediates **3** and **4** plays almost no role in a potential protonation event at the Pt atom.

As intermediate **4** is not an active species, the photocatalytic process has to be continued

by a second excitation process. According to Figure 1b, the maximum transition probability of intermediate **4** occurs at a wavelength that corresponds to a ^{2}MLCT excitation from the ruthenium metal center to the ligands. Thus the intersystem crossing (ISC) and vibrational cooling (VC) from the doublet into the quadruplet state becomes allowed,[61–63] forming intermediate **5**. This transition is associated with a significant increase of the pK_a for the second protonation step to roughly 14 both at the second pyrazine nitrogen atom and at the Pt center. However, the doubly protonated complex still only exists in very small concentrations since the pK_a values are still smaller by three units than that of $pK_a(NEt_3H^+)$.

The subsequent electron transfer from the NEt_3 reducing agent is slightly exergonic by -0.33 eV (Scheme 2). This results in the formation of a doubly reduced triplet state, intermediate **6**. According to the Mulliken charge analysis, the excess electron from the donor becomes located at the bridge site with a small spillover onto the catalyst. The pK_a of this doubly reduced intermediate increases slightly to 15.5 with a preference for protonation at the Pt site. This is already reasonably close to the pK_a of 17.6 of the proton donor and, thus, may allow for the presence of a minor concentration of the doubly protonated complex with one proton at the bridging ligand and one at the catalyst. The reaction energy for this proton transfer is slightly endergonic by 0.15 eV and associated with a moderate activation barrier of 0.66 eV (see Scheme S4). Therefore, the protonation of intermediate **6** can proceed at a slow rate. However, this Pt-H hydride is not yet active for hydrogen evolution since the H–H bond formation is still strongly endergonic by 1.48 eV (see Scheme S4). Thus, at least a third reduction is needed to facilitate hydrogen evolution. Similar observations have also been reported for the HER with $[(bpy)Rh(Cp^*)X]^{n+}$-based catalysts under non-acidic conditions.[64–68]

Interestingly, the higher intensity of the ^{2}MLCT transitions of intermediate **4** is crucial for the photocatalytic step. Assuming that the intra-ligand charge transfer (^{2}ILCT) and ligand to ligand charge transfer (^{2}LLCT) transitions have higher oscillator strengths than the ^{2}MLCT state, the intersystem crossing (ISC) process will be much slower and the reduction

Scheme 3: Possible reaction mechanism for the double protonation of the bridging ligand.

process would favor a doubly reduced singlet state, intermediate **13** (see Scheme S2 for details). The formation of a singlet spin state (intermediate **13**) renders the second nitrogen atom a stronger base compared to the preferred triplet state, i.e. the pK_a increases from 14.5 in intermediate 6 to 24.2 in intermediate 13. Accordingly, the bridging ligand would be doubly protonated under reaction conditions according to scheme 3. Thus, avoiding the low spin route by switching off ^{2}ILCT and ^{2}LLCT transitions[17,60] in Rxn IV is crucial for avoiding catalyst deactivation. It is noteworthy, that under electrochemical conditions which can only proceed through the more stable low spin states, this catalyst would therefore be subject to rapid deactivation.

The third reduction is initialized by a photoexcitation at 443 nm. After an intersystem crossing and vibrational cooling from the triplet to the quintet state, intermediate **7** is obtained. The excitation corresponds to a charge transfer from the Ru and partly the Pt center to the surrounding ligands (T45 and T50 in Figure 1c). The Mulliken charge analysis indicates an electron transfer of around 0.6e from the photosensitizer towards the bridging ligand. The triplet to quintet excitation results in a slight increase of the pK_a at the Pt site from 15.5 to 16.6, while at the same it decreases the pK_a of the second pyrazine nitrogen by a similar amount to 13.0. Thus, double protonation of the bridge is thermodynamically significantly less favorable. In addition, the higher basicity of the Pt-catalyst increases the concentration of the protonated Pt-H hydride species, which is important for the subsequent H_2 formation. The reaction energy for proton transfer is 0.07 eV with a moderate activation

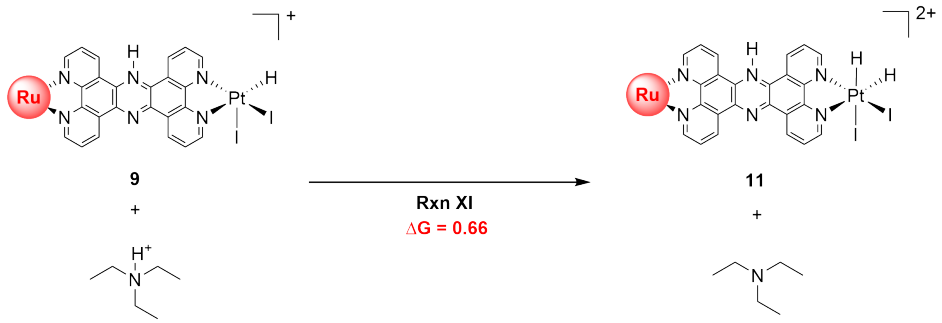

Scheme 4: Hypothetical scheme for the double protonation of the catalyst.

barrier of 0.54 eV. According to our calculations, the Pt atom is elevated towards the N–H bond of NEt_3H^+ to avoid steric interaction in the transition state (Scheme 2). Moreover, the protonation changes the coordination sphere around the Pt center from square planar to tetragonal bipyramidal with an iodide ligand in the axial position and the hydrogen atom in the planar position. The protonation is followed by a reduction of the complex through oxidation of NEt_3 with a change in Gibbs free energy of -0.03 eV to form intermediate **9**.

Intermediate **9** corresponds to the final state before the formation of molecular hydrogen occurs. As mentioned above, there are two possible pathways in the hydrogen formation process: the Volmer-Tafel and Volmer-Heyrovsky paths.[24–32] The necessary first steps of both mechanisms, the Volmer reaction, has already occurred at Rxn VII. In the Tafel mechanism, a second proton binds to the catalyst followed by the recombinative desorption of the two hydrogen atoms. According to rules of organometallic complex formation,[69] only the axial position can act as the available site for the second proton to form an octahedral conformation. However, the pK_a of the second proton at Pt is 8.4 (see intermediate **9** in Scheme 1) and thus, far too low to allow for the proton transfer from NEt_3H^+, which has a pK_a of 17.6 or Gibbs free energy of reaction of 0.66 eV according to scheme 4. Note that this is in analogy with the findings for the HER on platinum surfaces in heterogeneous catalysis where no PtH_2 complexes are found on Pt surfaces.[70]

The significant decrease of the pK_a compared to the first Pt-H bond is in good agreement with general trends for multiprotonic acids[69] and a result of the decrease in electron density

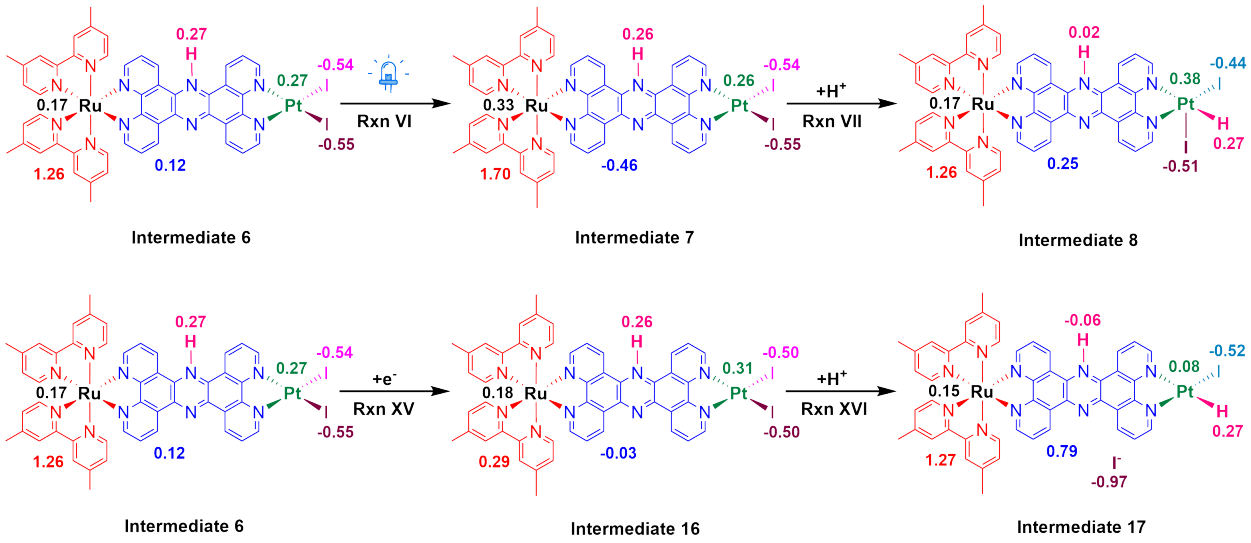

Figure 2: The Mulliken charge of intermediates in two reactions: catalyst activation (top) and loss of iodide ligand reaction (bottom).

at the bridging ligand and the Pt after the first protonation by 0.46e and 0.15e, respectively (see Rxn VII in Figure 2). Nevertheless, hydrogen evolution from such a doubly protonated species would be feasible as it requires only to overcome a moderate barrier of 0.50 eV. Overall, a direct Tafel like mechanism can be excluded for $RuPtI_2$, owing to the very low concentration of the doubly protonated species at the Pt center even though it is kinetically feasible.

This leaves only a Heyrovsky mechanism as the possible path to H_2 formation. Indeed, the direct attack of a proton at the Pt–H site is with 0.08 eV almost thermoneutral (see Rxn IX in Scheme 2). Additionally, the activation barrier of Rxn IX is 0.68 eV. The moderate barrier is associated with the planar position of the Pt–H hydride and the attack of NEt_3H^+ from the axial direction. This configuration allows for the stabilization of the H–H species through an interaction between the d-orbitals of Pt-atom and the σ bond of the H–H species. However, the steric interactions between the ethyl groups of NEt_3H^+ and the phenanthroline group of $RuPtI_2$ slow down the proton transfer. According to a Mulliken charge analysis, the proton transfer process and the formation of the H_2 molecules in Rxn IX require an electron transfer of 0.8e and 0.2e from the bridging ligand and the Pt-catalyst of intermediate **9**,

respectively. Overall, this indicates that the role of the bridging ligand is not only to connect the photosensitizer and catalyst but also to act as an electron storage before being used in the H_2 formation.[71]

Although molecular hydrogen is produced from intermediate **9**, deactivation can also occur at this intermediate. We find the second protonation step at the bridge to be associated with a pK_a of 15.0. This is reasonably close to the pK_a of the proton donor, NEt_3H^+, to allow for some double protonation of the bridge. Consequently, proton transfer is feasible here with a reaction slightly endergonic by 0.18 eV, but hindered by a rather high activation barrier of 0.82 eV. After formation of the protonated bridge species, hydrogen evolution is hindered by a very high activation barrier of 1.13 eV and is therefore effectively inhibited (see Scheme S10 for details). Although the reaction is slow, the deactivation process in $RuPtI_2$ cannot be avoided and may at least partly explain the experimentally observed catalyst deactivation after 48 hours of operation.[8,16–18,60]

Returning to the photocatalytic cycle shown in Scheme 1, we note that once the H–H bond is formed, H_2 is immediately released from the catalyst under formation of a trigonal pyramidal coordination sphere around Pt yielding intermediate **10**. According to a spin analysis (see Figure S2), the total spin on the bridging ligand and PtI_2 of intermediate **10** is 1.27 and 1.73, respectively. In other words, there is roughly one unpaired electron on the bridging ligand and two unpaired electrons on the PtI_2 catalyst due to the non-square planar configuration. Furthermore, the I–Pt–I configuration in $RuPtI_2$ is similar to the CO–Pt–Cl configuration in the triplet metal-centered (^{3}MC) state of Pt(ppy)(CO)(Cl) that were calculated by Escudero and coworkers.[72,73] Thus, intermediate **10** can be considered as a quartet metal centered (^{4}MC) state of $RuPtI_2$.[72,73] Afterward, the photocatalytic cycle ends with the restoration of its square planar coordination geometry (see Rxn X in Scheme 2). This restoration is followed by spin crossover from quartet to doublet,[72–75] forming intermediate **4**.

Besides the mechanism of the light-driven hydrogen evolution reaction (HER) of $RuPtI_2$, also the prevention of degradation is of high relevance and can be unraveled in our mechanistic

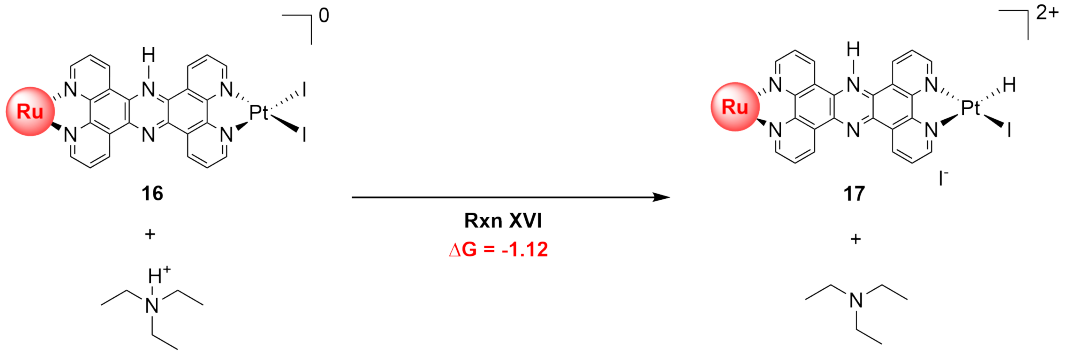

Scheme 5: Release of an I^- ligand from the catalyst upon protonation of the Pt site of intermediate **16**.

first-principles study. According to our calculations, the ability to access higher spin states through intersystem crossing avoids catalyst degradation, as shown for the conversion of intermediate **4** into **6**. Assume a situation in which, starting from intermediate **6**, the ^{3}ILCT and ^{3}LLCT transitions would have the highest harmonic oscillator strengths. Similar to the previous case this would again slow down the intersystem crossing and thus inhibit the transition into a quintet state. Accordingly, the more stable triply reduced doublet state, intermediate **16**, is formed. The Pt site of this species is strongly basic with a pK_a of 33.1. While this is to some degree even beneficial we also find that protonation of the Pt site in a doublet state immediately results in the release of an I^- ligand (intermediate **17** in scheme 5).

The degradation process in Rxn XVI can be explained by the changes in Mulliken charges in Figure 2. The release of the iodide ligand is initiated by the formation of intermediate **16** through an electron transfer. Here, excess electron density from the donor accumulates on the photosensitizer, specifically on the bipyridine ligand. One additional electron becomes stored at the $Rubpy_2$ unit in the doublet state compared to the quartet state. Upon Pt–H bond formation, 1.8e electrons are transferred from the bipyridine and bridging ligand to the active site. Of these electrons 0.7e are specifically utilized for proton reduction while the remaining electrons are allocated for the release of the iodide ligand as I^-. This result confirms findings from previous studies that the decomposition process in PtX_2 catalysts (where X = Cl and I)

occurs when the catalyst acquires two electrons.[76–78] On the other hand, catalyst degradation is not observed when only one electron is transferred to the catalyst. Note that the low spin decomposition path can again not be avoided under electrochemical conditions since it does not allow the excitation to the stable quartet state. Similarly, this path is also the preferred route if the bridging ligand would remain unprotonated. Hence, single protonation of the bridging ligand is critical for maintaining catalyst stability by deactivating the ILCT and LLCT transitions and allowing the ISC process to access the higher spin state which prevents degradation.

Another alternative to avoid degradation is utilizing the optical properties of intermediate **16** (see Scheme S8 for details). According to our TD-DFT calculations, the wavelength of maximum absorption of this intermediate at a value of 449 nm is characterized by a ^{2}MLCT (see Table S8 in the SI). Therefore, intersystem crossing from doublet to quadruplet is allowed to form intermediate **8**. Based on previous work,[16,17,61,79–82] the intersystem crossing in ruthenium complexes occurs rapidly with a timescale below 1 ps. Meanwhile, protonation at the Pt center occurs at a timescale above 1 ps,[83–85] depending on the reaction environment and proton concentration. Thus, the ISC process is much faster than protonation, and catalyst degradation on the triply reduced doublet state can be evaded through this excitation and the transition into the more stable quartet state. Indeed, the stability of the catalyst itself becomes a serious issue in Ru-Pt based catalysts with different bridging ligands, especially for ligands that cannot be protonated.[12,13,86–90]

Conclusions

In conclusion, based on state-of-the-art first-principles calculations we have presented a complete catalytic cycle of the photocatalytic hydrogen evolution reaction on a photochemical molecular device. To the best of our knowledge, such a complete catalytic cycle has not been reported before. The proposed reaction mechanism is fully consistent with all the ex-

perimental information where available. Our study clearly reveals the important role of the bridging ligand between photosensitizer and the catalyst in the hydrogen evolution reaction. It furthermore explains for the first time the previously not visible induction process for activating the photochemical molecular device. It highlights the correlation between light driven electron transfer from the photocenter to the bridging ligand and subsequent protonation of the bridging ligand. Only this step enables the formation of hydrogen at the later stages of the catalytic cycle. It furthermore shifts the perspective on this light driven catalytic process, as a doublet, or even higher multiplicity, ground state has to be taken into consideration for the investigation of these mechanisms.

The reaction proceeds through a threefold reduction followed by a Volmer-Heyrovsky type hydrogen evolution mechanism. The hydrogen molecule is eventually formed from a proton in solution and a hydrogen atom bound to the Pt-based catalyst together with an electron transfer both from the bridging ligand and the catalyst of the photomolecular device. This means that the bridging ligand also acts as an electron storage thus being directly involved in the hydrogen evolution reaction. Besides, it turns out that the single protonation of the bridging ligand is critical for maintaining catalyst stability. The atomic-level understanding of the crucial processes and steps in the photocatalytic hydrogen evolution reaction obtained in this quantum chemical study should be instrumental in further improving the activity of photomolecular devices.

Acknowledgments

Computer time on the JUSTUS cluster at Ulm University provided by the bwHPC initiative and the bwHPC-C5 project funded by the Baden-Württemberg government (MWK) and the German Research Foundation (DFG) is gratefully acknowledged. M.H.P., A.K.M., B.B., S.R., and A.G. thank the DFG for financial support through Project A1 and C5 of the Transregional Collaborative Research Centre TRR234 CataLight (Project No.364549901).

M.B. acknowledges financial support through the Dr. Barbara-Mez-Starck foundation and the Wallenberg Initiative Materials Science for Sustainability (WISE) funded by the Knut and Alice Wallenberg Foundation (KAW). This work contributes to the research performed at CELEST (Center for Electrochemical Energy Storage Ulm-Karlsruhe).

References

(1) Schlögl, R. The Role of Chemistry in the Energy Challenge. *ChemSusChem* **2010**, *3*, 209–222.

(2) Grätzel, M. Photoelectrochemical cells. *Nature* **2001**, *414*, 338–344.

(3) Dalle, K. E.; Warnan, J.; Leung, J. J.; Reuillard, B.; Karmel, I. S.; Reisner, E. Electro- and Solar-Driven Fuel Synthesis with First Row Transition Metal Complexes. *Chem. Rev.* **2019**, *119*, 2752–2875.

(4) Staffell, I.; Scamman, D.; Abad, A. V.; Balcombe, P.; Dodds, P. E.; Ekins, P.; Shah, N.; Ward, K. R. The role of hydrogen and fuel cells in the global energy system. *Energy Environ. Sci.* **2019**, *12*, 463–491.

(5) Li, G.; Zhu, D.; Wang, X.; Su, Z.; Bryce, M. R. Dinuclear metal complexes: multifunctional properties and applications. *Chem. Soc. Rev.* **2020**, *49*, 765–838.

(6) Andreiadis, E. S.; Chavarot-Kerlidou, M.; Fontecave, M.; Artero, V. Artificial Photosynthesis: From Molecular Catalysts for Light-driven Water Splitting to Photoelectrochemical Cells. *Photochem. Photobiol.* **2011**, *87*, 946–964.

(7) Costabel, D.; De, R.; Jacobi, F.; Eichhorn, J.; Hotzel, K.; Nabiyan, A.; Neumann, C.; Turchanin, A.; Kupfer, S.; Schacher, F. H.; Rau, S.; Dietzek-Ivanšić, B.; Peneva, K. Bridging Platinum and Palladium to Bipyridine-Annulated Perylene for Light-Driven Hydrogen Evolution. *ACS Catal.* **2023**, *13*, 7159–7169.

(8) Pfeffer, M. G.; Schäfer, B.; Smolentsev, G.; Uhlig, J.; Nazarenko, E.; Guthmuller, J.; Kuhnt, C.; Wächtler, M.; Dietzek, B.; Sundström, V.; Rau, S. Palladium versus Platinum: The Metal in the Catalytic Center of a Molecular Photocatalyst Determines the Mechanism of the Hydrogen Production with Visible Light. *Angew. Chem.* **2015**, *54*, 5044–5048.

(9) Putra, M. H.; Bagemihl, B.; Rau, S.; Groß, A. Prediction of Strong Solvatochromism in a Molecular Photocatalyst**. *Chem. Eur. J.* **2023**, *30*.

(10) Tschierlei, S.; Presselt, M.; Kuhnt, C.; Yartsev, A.; Pascher, T.; Sundström, V.; Karnahl, M.; Schwalbe, M.; Schäfer, B.; Rau, S.; Schmitt, M.; Dietzek, B.; Popp, J. Photophysics of an Intramolecular Hydrogen-Evolving Ru-Pd Photocatalyst. *Chem. Eur. J.* **2009**, *15*, 7678–7688.

(11) Sen, A.; Putra, M. H.; Biswas, A. K.; Behera, A. K.; Groß, A. Insight on the choice of sensitizers/dyes for dye sensitized solar cells: A review. *Dyes and Pigments* **2023**, *213*, 111087.

(12) Lämmle, M.; Mengele, A. K.; Shillito, G. E.; Kupfer, S.; Rau, S. Stability of Catalytic Centres in Light-Driven Hydrogen Evolution by Di- and Oligonuclear Photocatalysts. *Chem. Eur. J.* **2023**, *29*.

(13) Lämmle, M.; Pilz, T. D.; Kutta, R. J.; Mißler, M.; Mengele, A. K.; Görls, H.; Heinemann, F. W.; Rau, S. Insights into the different mechanistic stages of light-induced hydrogen evolution of a 5, 5'-bisphenanthroline linked RuPt complex. *Dalton Trans.* **2022**, *51*, 15282–15291.

(14) Zedler, L.; Guthmuller, J.; Rabelo de Moraes, I.; Kupfer, S.; Krieck, S.; Schmitt, M.; Popp, J.; Rau, S.; Dietzek, B. Resonance-Raman spectro-electrochemistry of intermediates in molecular artificial photosynthesis of bimetallic complexes. *Chem. Commun.* **2014**, *50*, 5227.

(15) Giannoudis, E.; Bold, S.; Müller, C.; Schwab, A.; Bruhnke, J.; Queyriaux, N.; Gablin, C.; Leonard, D.; Saint-Pierre, C.; Gasparutto, D.; Aldakov, D.; Kupfer, S.; Artero, V.; Dietzek, B.; Chavarot-Kerlidou, M. Hydrogen Production at a NiO Photocathode Based on a Ruthenium Dye–Cobalt Diimine Dioxime Catalyst Assembly: Insights from Advanced Spectroscopy and Post-operando Characterization. *ACS Appl. Mater. Interfaces* **2021**, *13*, 49802–49815.

(16) Pfeffer, M. G.; Kowacs, T.; Wächtler, M.; Guthmuller, J.; Dietzek, B.; Vos, J. G.; Rau, S. Optimization of Hydrogen-Evolving Photochemical Molecular Devices. *Angew. Chem. Int.* **2015**, *54*, 6627–6631.

(17) Pfeffer, M. G. et al. Active repair of a dinuclear photocatalyst for visible-light-driven hydrogen production. *Nat. Chem.* **2022**, *14*, 500–506.

(18) Klingler, S.; Bagemihl, B.; Mengele, A. K.; Kaufhold, S.; Myllyperkiö, P.; Ahokas, J.; Pettersson, M.; Rau, S.; Mizaikoff, B. Rationalizing In Situ Active Repair in Hydrogen Evolution Photocatalysis via Non-Invasive Raman Spectroscopy. *Angew. Chem., Int. Ed.* **2023**, *62*.

(19) Martynow, M.; Kupfer, S.; Rau, S.; Guthmuller, J. Excited state properties of a series of molecular photocatalysts investigated by time dependent density functional theory. *Phys. Chem. Chem. Phys.* **2019**, *21*, 9052–9060.

(20) Staniszewska, M.; Kupfer, S.; Guthmuller, J. Effect of the Catalytic Center on the Electron Transfer Dynamics in Hydrogen-Evolving Ruthenium-Based Photocatalysts Investigated by Theoretical Calculations. *J. Phys. Chem. C* **2019**, *123*, 16003–16013.

(21) Müller, C.; Friedländer, I.; Bagemihl, B.; Rau, S.; Dietzek-Ivanšić, B. The electron that breaks the catalyst's back - excited state dynamics in intermediates of molecular photocatalysts. *Phys. Chem. Chem. Phys.* **2021**, *23*, 27397–27403.

(22) Ozawa, H.; Sakai, K. Photo-hydrogen-evolving molecular devices driving visible-light-induced water reduction into molecular hydrogen: structure–activity relationship and reaction mechanism. *Chem. Commun.* **2011**, *47*, 2227.

(23) Ogawa, M.; Ajayakumar, G.; Masaoka, S.; Kraatz, H.; Sakai, K. Platinum(II)-Based Hydrogen-Evolving Catalysts Linked to Multipendant Viologen Acceptors: Experimental and DFT Indications for Bimolecular Pathways. *Chem. Eur. J.* **2010**, *17*, 1148–1162.

(24) Erdey-Grúz, T.; Volmer, M. Zur Theorie der Wasserstoff Überspannung. *Zeitschrift für Physikalische Chemie* **1930**, *150A*, 203–213.

(25) Tafel, J. Über die Polarisation bei kathodischer Wasserstoffentwicklung. *Zeitschrift für Physikalische Chemie* **1905**, *50U*, 641–712.

(26) Heyrovský, J. A theory of overpotential. *Recueil des Travaux Chimiques des Pays-Bas* **1927**, *46*, 582–585.

(27) Schnur, S.; Groß, A. Challenges in the first-principles description of reactions in electrocatalysis. *Catal. Today* **2011**, *165*, 129–137.

(28) Huang, J.; Zhu, X.; Eikerling, M. The rate-determining term of electrocatalytic reactions with first-order kinetics. *Electrochim. Acta* **2021**, *393*, 139019.

(29) Kronberg, R.; Lappalainen, H.; Laasonen, K. Revisiting the Volmer–Heyrovský mechanism of hydrogen evolution on a nitrogen doped carbon nanotube: constrained molecular dynamics versus the nudged elastic band method. *Phys. Chem. Chem. Phys.* **2020**, *22*, 10536–10549.

(30) Chen, Z.; Duan, X.; Wei, W.; Wang, S.; Ni, B.-J. Recent advances in transition metal-based electrocatalysts for alkaline hydrogen evolution. *J. Mater. Chem. A* **2019**, *7*, 14971–15005.

(31) Faid, A. Y.; Sunde, S. Anion Exchange Membrane Water Electrolysis from Catalyst Design to the Membrane Electrode Assembly. *Energy Technol.* **2022**, *10*.

(32) Wu, Z.-P.; Lu, X. F.; Zang, S.-Q.; Lou, X. W. D. Non-Noble-Metal-Based Electrocatalysts toward the Oxygen Evolution Reaction. *Adv. Funct. Mater.* **2020**, *30*.

(33) Lasia, A. Mechanism and kinetics of the hydrogen evolution reaction. *Int. J. Hydrogen Energy* **2019**, *44*, 19484–19518.

(34) Frisch, M. J. et al. Gaussian16 Revision C.01. 2016; Gaussian Inc. Wallingford CT.

(35) Becke, A. D. Density functional thermochemistry. III. The role of exact exchange. *J. Chem. Phys.* **1993**, *98*, 5648–5652.

(36) Lee, C.; Yang, W.; Parr, R. G. Development of the Colle-Salvetti correlation-energy formula into a functional of the electron density. *Phys. Rev. B* **1988**, *37*, 785–789.

(37) Grimme, S.; Ehrlich, S.; Goerigk, L. Effect of the damping function in dispersion corrected density functional theory. *J. Comp. Chem.* **2011**, *32*, 1456–1465.

(38) Weigend, F.; Ahlrichs, R. Balanced basis sets of split valence, triple zeta valence and quadruple zeta valence quality for H to Rn: Design and assessment of accuracy. *Phys. Chem. Chem. Phys.* **2005**, *7*, 3297–3305.

(39) Weigend, F. Accurate Coulomb-fitting basis sets for H to Rn. *Phys. Chem. Chem. Phys.* **2006**, *8*, 1057–1065.

(40) Groß, A. Challenges for ab initio molecular dynamics simulations of electrochemical interfaces. *Current Opinion in Electrochemistry* **2023**, *40*, 101345.

(41) Marenich, A. V.; Cramer, C. J.; Truhlar, D. G. Universal Solvation Model Based on Solute Electron Density and on a Continuum Model of the Solvent Defined by the Bulk Dielectric Constant and Atomic Surface Tensions. *J. Phys. Chem. B* **2009**, *113*, 6378–6396.

(42) Adamo, C.; Jacquemin, D. The calculations of excited-state properties with Time-Dependent Density Functional Theory. *Chem. Soc. Rev.* **2013**, *42*, 845–856.

(43) Laurent, A. D.; Adamo, C.; Jacquemin, D. Dye chemistry with time-dependent density functional theory. *Phys. Chem. Chem. Phys.* **2014**, *16*, 14334–14356.

(44) Busch, M.; Ahlberg, E.; Laasonen, K. From absolute potentials to a generalized computational standard hydrogen electrode for aqueous and non-aqueous solvents. *Phys. Chem. Chem. Phys.* **2021**, *23*, 11727–11737.

(45) Busch, M.; Ahlberg, E.; Ahlberg, E.; Laasonen, K. How to Predict the pK_a of Any Compound in Any Solvent. *ACS Omega* **2022**, *7*, 17369–17383.

(46) Busch, M.; Ahlberg, E.; Laasonen, K. Universal Trends between Acid Dissociation Constants in Protic and Aprotic Solvents. *Chem. Eur. J.* **2022**, *28*.

(47) Ho, J.; Coote, M. L. pKa Calculation of Some Biologically Important Carbon Acids - An Assessment of Contemporary Theoretical Procedures. *J. Chem. Theory Comput.* **2009**, *5*, 295–306.

(48) Ho, J. Predicting pKa in Implicit Solvents: Current Status and Future Directions. *Aust. J. Chem.* **2014**, *67*, 1441.

(49) Casasnovas, R.; Ortega-Castro, J.; Frau, J.; Donoso, J.; Muñoz, F. Theoretical pKa calculations with continuum model solvents, alternative protocols to thermodynamic cycles. *Int. J. Quantum Chem.* **2014**, *114*, 1350–1363.

(50) Ho, J.; Coote, M. L. A universal approach for continuum solvent pK a calculations: are we there yet? *Theor. Chem. Acc.* **2009**, *125*, 3–21.

(51) Muckerman, J. T.; Skone, J. H.; Ning, M.; Wasada-Tsutsui, Y. Toward the accurate calculation of pKa values in water and acetonitrile. *Biochim. Biophys. Acta* **2013**, *1827*, 882–891.

(52) Rossini, E.; Knapp, E.-W. Proton solvation in protic and aprotic solvents. *J. Comput. Chem.* **2016**, *37*, 1082–1091.

(53) Busch, M.; Laasonen, K.; Ahlberg, E. Method for the accurate prediction of electron transfer potentials using an effective absolute potential. *Phys. Chem. Chem. Phys.* **2020**, *22*, 25833–25840.

(54) Tshepelevitsh, S.; Kütt, A.; Lõkov, M.; Kaljurand, I.; Saame, J.; Heering, A.; Plieger, P. G.; Vianello, R.; Leito, I. On the Basicity of Organic Bases in Different Media. *European Journal of Organic Chemistry* **2019**, *2019*, 6735–6748.

(55) Pellegrin, Y.; Odobel, F. Sacrificial electron donor reagents for solar fuel production. *C. R. Chimie* **2016**, *20*, 283–295.

(56) Cline, E. D.; Adamson, S. E.; Bernhard, S. Homogeneous Catalytic System for Photoinduced Hydrogen Production Utilizing Iridium and Rhodium Complexes. *Inorg. Chem.* **2008**, *47*, 10378–10388.

(57) Smith, P. J.; Mann, C. K. Electrochemical dealkylation of aliphatic amines. *J. Org. Chem.* **1969**, *34*, 1821–1826.

(58) DeLaive, P. J.; Foreman, T. K.; Giannotti, C.; Whitten, D. G. Photoinduced electron transfer reactions of transition-metal complexes with amines. Mechanistic studies of alternate pathways to back electron transfer. *J. Am. Chem. Soc.* **1980**, *102*, 5627–5631.

(59) Whitten, D. G. Photoinduced electron transfer reactions of metal complexes in solution. *Acc. Chem. Res.* **1980**, *13*, 83–90.

(60) Pfeffer, M. G.; Kowacs, T.; Wächtler, M.; Guthmuller, J.; Dietzek, B.; Vos, J. G.; Rau, S. Optimization of Hydrogen-Evolving Photochemical Molecular Devices. *Angew. Chem., Int. Ed.* **2015**, *54*, 6627–6631.

(61) Zedler, L.; Kupfer, S.; Schmidt, H.; Dietzek-Ivanšić, B. Oxidation-state sensitive light-induced dynamics of Ruthenium-4H-Imidazole complexes. *Chemistry – A European Journal* **2024**, *30*.

(62) Yoshimura, A.; Torieda, H.; Ohno, T. Doublet-Quartet Intersystem Crossing and Electron Transfer of Cobalt(II) Moieties in [LRuIII(L-L)CoIIL]5+ (L = 2, 2':6', 2"-Terpyridine and L-L = A Bridging Ligand). *J. Phys. Chem. A* **2004**, *108*, 2149–2154.

(63) Barral, M. C.; Casanova, D.; Herrero, S.; Jiménez-Aparicio, R.; Torres, M. R.; Urbanos, F. A. Tuning the Magnetic Moment of [Ru2(DPhF)3(O2CMe)L]+ Complexes (DPhF=N, N'-Diphenylformamidinate): A Theoretical Explanation of the Axial Ligand Influence. *Chem. Eur. J.* **2010**, *16*, 6203–6211.

(64) Caix, C.; Chardon-Noblat, S.; Deronzier, A.; Moutet, J.-C.; Tingry, S. (Pentamethylcyclopentadienyl)(polypyridyl) rhodium and iridium complexes as electrocatalysts for the reduction of protons to dihydrogen and the hydrogenation of organics. *J. Organomet. Chem.* **1997**, *540*, 105–111.

(65) Henke, W. C.; Lionetti, D.; Moore, W. N. G.; Hopkins, J. A.; Day, V. W.; Blakemore, J. D. Ligand Substituents Govern the Efficiency and Mechanistic Path of Hydrogen Production with [Cp*Rh] Catalysts. *ChemSusChem* **2017**, *10*, 4589–4598.

(66) Quintana, L. M. A.; Johnson, S. I.; Corona, S. L.; Villatoro, W.; Goddard, W. A.; Takase, M. K.; VanderVelde, D. G.; Winkler, J. R.; Gray, H. B.; Blakemore, J. D. Proton–hydride tautomerism in hydrogen evolution catalysis. *Proc. Natl. Acad. Sci. U. S. A.* **2016**, *113*, 6409–6414.

(67) Henke, W. C.; Peng, Y.; Meier, A. A.; Fujita, E.; Grills, D. C.; Polyansky, D. E.; Blakemore, J. D. Mechanistic roles of metal- and ligand-protonated species in hydrogen evolution with [Cp*Rh] complexes. *Proc. Natl. Acad. Sci. U. S. A.* **2023**, *120*.

(68) Johnson, S. I.; Gray, H. B.; Blakemore, J. D.; Goddard, W. A. Role of Ligand Protonation in Dihydrogen Evolution from a Pentamethylcyclopentadienyl Rhodium Catalyst. *Inorg. Chem.* **2017**, *56*, 11375–11386.

(69) Holleman, A. F.; und Nils Wiberg, E.; Fischer, G. *Lehrbuch der Anorganischen Chemie*; Walter de Gruyter, 2007.

(70) Lischka, M.; Groß, A. Hydrogen adsorption on an open metal surface:H_2/Pd(210). *Physical Review B* **2002**, *65*.

(71) Whang, D. R.; Park, S. Y. Rational Design of an Electron-Reservoir PtII Complex for Efficient Photocatalytic Hydrogen Production from Water. *ChemSusChem* **2015**, *8*, 3204–3207.

(72) Escudero, D.; Thiel, W. Exploring the Triplet Excited State Potential Energy Surfaces of a Cyclometalated Pt(II) Complex: Is There Non-Kasha Emissive Behavior? *Inorg. Chem.* **2014**, *53*, 11015–11019.

(73) Kumar, P.; Escudero, D. Computational Protocol to Calculate the Phosphorescence Energy of Pt(II) Complexes: Is the Lowest Triplet Excited State Always Involved in Emission? A Comprehensive Benchmark Study. *Inorg. Chem.* **2021**, *60*, 17230–17240.

(74) Shillito, G. E.; Rau, S.; Kupfer, S. Plugging the 3MC Sink in RuII-Based Photocatalysts. *ChemCatChem* **2023**, *15*.

(75) Hernandez-Castillo, D.; Nau, R. E. P.; Schmid, M.; Tschierlei, S.; Rau, S.; Gonzalez, L. Multiple Triplet Metal-Centered Jahn-Teller Isomers Determine Temperature-Dependent Luminescence Lifetimes in [Ru(bpy)3]2+. *Angew. Chem.* **2023**, *62*.

(76) Whang, D. R.; Park, S. Y. Rational Design of an Electron-Reservoir Pt^{II} Complex for Efficient Photocatalytic Hydrogen Production from Water. *ChemSusChem* **2015**, *8*, 3204–3207.

(77) Collison, D.; Mabbs, F. E.; McInnes, E. J. L.; Taylor, K. J.; Welch, A. J.; Yellowlees, L. J. Electrochemical and spectroelectrochemical studies on platinum complexes containing 2, 2'-bipyridine. *J. Chem. Soc.* **1996**, 329–334.

(78) Yang, L.; Wimmer, F. L.; Wimmer, S.; Zhao, J.; Braterman, P. S. Electro- and spectroelectrochemistry of platinum(II) bipyridine complexes and related species. *J. Organomet. Chem.* **1996**, *525*, 1–8.

(79) Mengele, A. K.; Müller, C.; Nauroozi, D.; Kupfer, S.; Dietzek, B.; Rau, S. Molecular Scylla and Charybdis: Maneuvering between pH Sensitivity and Excited-State Localization in Ruthenium Bi(benz)imidazole Complexes. *Inorg. Chem.* **2020**, *59*, 12097–12110.

(80) Müller, C.; Schwab, A.; Randell, N. M.; Kupfer, S.; Dietzek-Ivanšić, B.; Chavarot-Kerlidou, M. A Combined Spectroscopic and Theoretical Study on a Ruthenium Complex Featuring a π-Extended dppz Ligand for Light-Driven Accumulation of Multiple Reducing Equivalents. *Chem. Eur. J.* **2022**, *28*.

(81) Schindler, J.; Traber, P.; Zedler, L.; Zhang, Y.; Lefebvre, J.-F.; Kupfer, S.; Gräfe, S.; Demeunynck, M.; Chavarot-Kerlidou, M.; Dietzek, B. Photophysics of a Ruthenium Complex with a π-Extended Dipyridophenazine Ligand for DNA Quadruplex Labeling. *J. Phys. Chem. A* **2018**, *122*, 6558–6569.

(82) Zedler, L.; Mengele, A. K.; Ziems, K. M.; Zhang, Y.; Wächtler, M.; Gräfe, S.; Pascher, T.; Rau, S.; Kupfer, S.; Dietzek, B. Unraveling the Light-Activated Reaction Mechanism in a Catalytically Competent Key Intermediate of a Multifunctional Molecular Catalyst for Artificial Photosynthesis. *Angew. Chem.* **2019**, *58*, 13140–13148.

(83) Barker, G. C.; Sammon, D. C. Kinetics of Proton-transfer Reactions. *Nature* **1967**, *213*, 65–66.

(84) Kornyshev, A. A.; Kuznetsov, A. M.; Spohr, E.; Ulstrup, J. Kinetics of Proton Transport in Water. *J. Phys. Chem. B* **2003**, *107*, 3351–3366.

(85) Montgomery, C. L.; Amtawong, J.; Jordan, A. M.; Kurtz, D. A.; Dempsey, J. L. Proton transfer kinetics of transition metal hydride complexes and implications for fuel-forming reactions. *Chem. Soc. Rev.* **2023**, *52*, 7137–7169.

(86) Lämmle, M.; Volk, S.; Klinkerman, M.; Müßler, M.; Mengele, A. K.; Rau, S. Efficient Access of Phenyl-Spaced 5, 5'-Bridged Dinuclear Ruthenium Metal Complexes and the Effect of Dynamic Ligand Exchange on Catalysis. *Photochem* **2022**, *2*, 831–848.

(87) Yamauchi, K.; Masaoka, S.; Sakai, K. Stability of Pt(ii)-based H2-evolving catalysts against H2 in aqueous solution. *Dalton Trans.* **2011**, *40*, 12447.

(88) Ozawa, H.; aki Haga, M.; Sakai, K. A Photo-Hydrogen-Evolving Molecular Device Driving Visible-Light-Induced EDTA-Reduction of Water into Molecular Hydrogen. *J. Am. Chem. Soc.* **2006**, *128*, 4926–4927.

(89) Sakai, K.; Ozawa, H. Homogeneous catalysis of platinum(II) complexes in photochemical hydrogen production from water. *Coord. Chem. Rev.* **2007**, *251*, 2753–2766.

(90) Lei, P.; Hedlund, M.; Lomoth, R.; Rensmo, H.; Johansson, O.; Leif, **2007**, *130*, 26–27.

Supplementary Files

This is a list of supplementary files associated with this preprint. Click to download.

- HERRuPtI22025submSI.pdf